ISBN 978-979-18839-0-0

Effect of Material Non-homogeneity on Fracture Toughness (Effect of Temperature Gradient)

Hiroomi Homma[1], Hisashi Nakamoto[2], and Yasuhiro Kanto[3]
[1]International Cooperation Center for Engineering Education Development, Toyohashi University of Technology 1-1 Tempaku-cho Toyohashi 441-8580 Japan, Tel.+(81) 532-44-6939
[2]IKobelco Kaken Ltd.
[3]Department of Mechanical Engineering, Ibaraki University
[1]homma@icceed.tut.ac.jp

Abstrak

The numerical analysis was performed to estimate the effect of material non-homogeneity induced by a temperature gradient on fracture toughness for SM490A steel. The temperature gradient in the specimen creates change in plastic properties at a position to the position to bring about non-homogeneity in the specimen. The experimental result shows the material non-homogeneity tends to change the fracture toughness from the expected one for the crack tip material properties. In the numerical analysis, void volume fraction was used for a dimple fracture criterion, and a set of critical values of plastic strain, stress tri-axiality and principal stress was taken as a cleavage fracture criterion. The stress and strain distributions at the same J-integral are different between the homogeneous and non-homogeneous materials. The numerical results agreed with the experimental result that the material non-homogeneity induced by the temperature gradient has a significant effect on the fracture toughness.

Keywords: Material Non-homogeneity, Fracture Criterion, Ductile Fracture, Brittle Fracture, Fracture Toughness, Finite Element Method, J-integral

1. Introduction

Recently, demands toward high performance and saving energy of structures and machines lead to development of new materials to be used for such structures and machines. As one promising material for those structures and machines operated under sever conditions, a functionally graded material (FGM) receives much attention. Therefore, FGM must be examined to evaluate its strength properties based on fracture mechanics. Many theoretical investigations[1-6] and numerical approaches[7-12] were carried out. Very limited experimental works were carried out because of technical difficulty in production of large sized specimens, whereas as mentioned above, many theoretical and numerical investigations were carried out. In addition, all of the works mentioned above dealt with elastic problems and almost none of works dealt with elasto-plastic problems.

FGM is non-homogeneous since the material property changes from the front surface to the back surface. Fracture toughness test of non-homogeneous materials were carried out by Homma et al[13]. In this test, non-homogeneity of material was created by temperature gradient in the steel specimen, because plastic properties of steel depend on temperature. The experimental result showed that fracture toughness of the non-homogeneous material differed from that of the material at the uniform temperature. This suggests that the stress and strain fields ahead of the crack are not expressed precisely by HHR field of J integral experimentally evaluated, but significantly affected by the material non-homogeneity.

To confirm this suggestion, an approach based on the microscopic fracture mechanism may be effective. Therefore, this work aims to discuss the effect of the material non-homogeneity from the aspect of microscopic fracture mechanism. Then, fracture toughness tests are carried out for non-homogeneous materials and experimental results are analyzed through stress and strain components obtained by finite element analysis.

2. Fracture Toughness Test

2.1 Material and Experimental Procedure

Material used for the experiment is steel for welding structure JIS SM490A. Chemical compositions and mechanical property are shown in Tables 1 and 2.

Table 1 Chemical compositions of JIS SM490A

C	Mn	Si	S	P
0.18	1.49	0.36	0.03	0.01

Table 2 Mechanical property of JIS SM490A

Test Temperature (°C)	Yield strength (MPa)	Ultimate strength (MPa)	Elongation (%)
20	304	490	17

Standard compact-tension type of specimen was used for the test and cut in the LT orientation of 30mm thick, 130mm wide and 2600mm long rolled plate. The specimen size was based on ASTM Standard E1820-01 and the specimen thickness was one inch and the ratio of the specimen width to the thickness W/B was 4.0. A fatigue pre-crack was introduced from the notch root so that the total crack length was 0.50 to 0.52 in the ratio to the specimen width.

In this test, a temperature gradient was introduced ahead of the crack tip so that fracture toughness could steeply change in the temperature range, similarly to the test by H. Homma et al[13]. The temperature dependence of fracture toughness for SM490A was measured by H. Nakamoto et al[14]. Referring to this result, the temperature was set at – 45 □, because non-homogeneity of material property associated with fracture toughness could be intensified in a small temperature change.
For the temperature gradient test, a apparatus shown in Fig. 1 was fabricated.. The apparatus consists of a cooling system and a heating system. The cooling system circulated isopentane (2-methyl butane, coagulation point:-160 °C) to cool down the notch-mouth end of the specimen using a magnet pump as shown in Fig. 1.

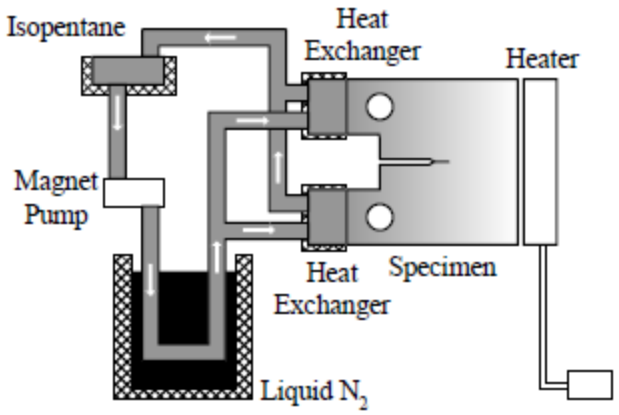

Fig. 1 Experimental schematic.

The isopentane was cooled down to -120 °C during flowing in copper pipe immersed in the liquid nitrogen tank. The heating system consists of nichrome wire and power supply. The end of the specimen was heated by radiated Joule heat of nichrome wire. The temperature of nichrome wire was adjusted by a transformer. The specimen surface and the pipe of isopenthane were covered by styrene foam for thermal isolation. The temperature was measured by thermo-couples mounted at five points with a constant interval on the specimen surface.

In the fracture toughness test, the temperature at the crack tip was fixed at -45 °C and the temperature gradient of 1°C/mm was generated ahead of the crack tip. The temperature distribution was almost linear across the specimen width. This temperature gradient is around five times as large as the gradient generated by the H. Homma et al test[13] and it can be expected that a significant effect of material non-homogeneity appears on fracture toughness.

According to H. Nakamoto et al fracture toughness test under a uniform temperature[14], SM490 steel was fractured in a cleavage mode at -45 °C. If the cleavage unstable fracture takes place in a

temperature gradient test, the fracture toughness is evaluated by ASTM 1820-01 standard test method. This standard test method provides the size requirement for plane strain fracture toughness as follows:

$$B,\ b_0 \geq (50 \sim 100)\frac{J_C}{\sigma_Y} \qquad (1)$$

Where B is the specimen thickness, b_0 is the ligament, J_C is the critical J-integral for the crack initiation, and σ_Y is the yield strength of the material. SM490 steel fractures in dimple mode caused by micro-void coalescence and cleave mode in the usual temperature range. When the microscopic fracture mode is transformed to the dimple mode, the evaluation of the fracture toughness is conducted by JSME S 001 standard method (Stretched zone method), because the standard method can evaluate the toughness at the crack initiation moment, whereas the ASTM standard test method evaluates the toughness after a certain amount of stable crack growth.

Fracture toughness test was conducted under the displacement control using a hydro-servo material testing machine (load capacity of 98 kN). Temperature of the specimen was controlled within ± 1 ^{o}C and after a specified temperature distribution was attained in the specimen and kept for 30 minutes, the fracture toughness test was conducted. After the test, fracture surfaces were observed by a scanning electron microscope to examine the microscopic fracture mechanisms and dispersion density of inclusions.

2.2 Experimental Results

Measured temperatures are plotted as a function of the distance from the crack tip for four specimens in Fig. 2. As seen, the temperature distributions are consistent for four specimens and linear ahead of the crack tip. The temperature is around - 45 ^{o}C at the crack tip and 10 ^{o}C at the ligament edge.

Observation of fracture surface after the fracture toughness test showed that all the specimens were fractured in an unstable manner by the cleavage fracture mechanism. Therefore, fracture toughness J_C was evaluated by ASTM standard test method E1820-01. However, because non-homogeneity of the material is introduced by the temperature distribution in the specimen, the measured toughness values are apparent ones. Those are summarized in Table 3. After the toughness test, the fracture surfaces were observed by the scanning electron microscope. The observation results showed that similarly to the fracture toughness test under the uniform temperature of -45 ^{o}C[14], dimple fracture took place at the crack tip in some specimens. The fracture toughness evaluated at the temperature gradient test is compared with the toughness under the uniform temperature test in Fig.3.

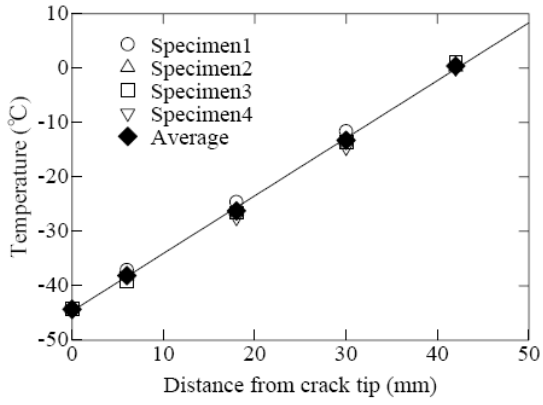

Fig.2 Temperature distribution in specimens

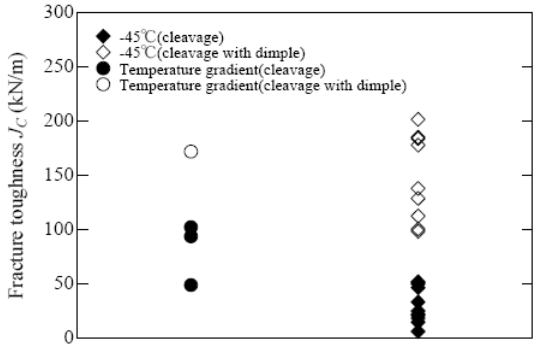

Fig.3 Comparison between fracture toughness values by uniform temperature test and by temperature gradient test

Table 3 Fracture toughness values by temperature gradient tests

Specimen	J_C (kN/m)	Microscopic Fracture Mechanism
No.1	49.2	Cleavage
No.2	94.0	Cleavage
No.3	102.5	Cleavage
No.4	172.1	Cleavage + Dimple

As seen in Fig.3, toughness results are scattered widely, because the temperature in the vicinity of the crack tip is inside of the transition temperature range for both the uniform temperature material and the temperature gradient material. Therefore, the effect of material non-homogeneity on the fracture toughness must be carefully discussed paying attention onto the microscopic fracture mechanism. As shown in Fig.3, in case where the fracture mode is transformed from dimple at the initiation to cleavage at the unstable growth, the results are scatted widely in the uniform temperature test, whereas only one data was obtained in the temperature gradient test. Thus, comparison between the above results cannot deduce a meaningful conclusion in engineering sense. In case where the cleavage fracture mode is directly operated from the fatigue pre-crack tip, the meaningful comparison between the results obtained by both the tests is possible. Simple average of measured toughness values are calculated as 29.3 kN/m and 81.9 kN/m for the uniform temperature test and the temperature gradient test, respectively. As though the results are scattered widely, the difference of the averaged toughness values is significant.

In the previous test[13], the cleavage fracture at the crack initiation was not observed for the temperature gradient material. It results from the difference in the tested material. The A533B steel used in the previous test is high quality one, and impurity and inclusion density is much low as compared with SM490 A steel.

3. Fracture Criterion

In the previous paper[14], fracture toughness test was conducted under different uniform temperatures to determine the fracture criteria for dimple and cleavage through the simulation of the observed crack initiation and growth by the finite element method. Using these fracture criteria, it was possible to estimate the wide variation in fracture toughness values in the range of the transient temperature. Fracture toughness for non-homogeneous material induced by the temperature gradient is estimated by the same numerical procedures as the fracture toughness at the uniform temperature. In this section, the used fracture criteria will be briefly explained.

Different sizes of inclusions are scattered in SM490A steel, but in finite element analysis, a typical size of inclusion is introduced. This inclusion is a main cause for a void nucleation. Two mechanisms are considered for the void nucleation. In the first mechanism, a void is nucleated by debonding of the interface between the inclusion and the matrix material when the plastic strain ε_p at the boundary exceeds a critical value. In the second mechanism, a void is nucleated by fracture of the inclusion

when the principal stress σ_0 exceed the critical value. The numerical analysis deals with dimple fracture, cleavage fracture, and void nucleation as follows. When a void volume fraction f in the element ahead of the crack tip reaches the critical value of 0.2, the dimple fracture takes place in the element and the element is deleted from the mesh model. The elastic-plastic fracture toughness J_C is defined as the condition where the void nucleated at the inclusion boundary and the crack tip coalesce as a result of the sequent dimple fracture of the elements ahead of the crack tip. The cleavage fracture is initiated when the next three conditions are simultaneously satisfied at a certain element ahead of the crack tip: plastic strain ε_p exceeds 0.00728; stress tri-axiality σ_m/σ_{eq} exceeds 2.5 where σ_m is mean stress and σ_{eq} is von Mises equivalent stress; and the principal stress exceeds 1700MPa. A main void is nucleated at the inclusion boundary when the plastic strain ε_p at the inclusion boundary exceeds 0.00916, or the principal stress σ_0 in the inclusion exceeds 1630 MPa. For simplicity, the mechanical property of the inclusion is assumed to be the same as that of the matrix steel. In the analysis, the elements forming the inclusion are eliminated to nucleate a void when either of the two void nucleation criteria mentioned above is satisfied.

4. Fracture Simulation in a Non-homogeneous Material

4.1 Analytical Method

The temperature in the specimens used for the experiment varies from 10 ^{o}C to 120 ^{o}C. The temperature dependence of mechanical property of SM490A steel was not measured, but the tensile test results for the similar steel by Wang[15] are utilized for the analysis. Material constants depending on the temperature are yield strength σ_Y, strain hardening exponent N, and plastic modulus C. Young's modulus E and Poisson's ratio υ are independent of the temperature and 206 GPa and 0.3, respectively. The material constitution equation is defined as

$$\sigma \le \sigma_Y, \quad \varepsilon = \frac{\sigma}{E}$$

$$\sigma \ge \sigma_Y, \quad \varepsilon = \frac{\sigma}{E} + \left[\left(\frac{\sigma}{C} \right)^N - \left(\frac{\sigma_Y}{C} \right)^N \right] \tag{2}$$

Material constants depending on the temperature in the above equation are expressed as follows:

$$\left.\begin{aligned} \sigma_Y &= 6.57\times10^{-5}T^3 + 1.23\times10^{-2}T^2 - 5.52\times10^{-1}T + 369 \\ \frac{1}{N} &= -4.71\times10^{-9}T^3 - 1.92\times10^{-6}T^2 - 2.97\times10^{-5}T + 0.214 \\ C &= 8.41\times10^{-4}T^3 + 9.04\times10^{-2}T^2 - 2.0\times T + 925 \end{aligned}\right\| \tag{3}$$

where T is the temperature in centigrade.

To monitor a void volume fraction in an element, the Tvergaard[16,17] material model(hereafter, called the modified Gusron material model) is used for the analysis as shown in the following equation:

$$\frac{\sigma_{eq}^2}{\sigma_Y^2} + 2q_1 f \cosh\left(\frac{3q_2\sigma_m}{2\sigma_Y} \right) - 1 - q_3 f^2 = 0 \tag{4}$$

where $\sigma_{eq} = \left({}^{3}\!/_{2\sigma_{ij}'} : \sigma_{ij}' \right)^{1/2}$, σ_{ij}' is deviation of stress component σ_{ij}, f is the volume fraction of micro-voids. q_1, q_2 and q_3 are fitting parameters to get good agreement between the

experimental result and the predicted one by the modified Gurson material model. The volume fraction of micro-voids is related with void nucleation and growth, and the void growth rate $\dot{f}_{nucl}$ is controlled by plastic strain as shown by the following equation:

$$\dot{f}_{nucl} = A\dot{\bar{\varepsilon}}_m^{pl},$$
$$A = \frac{f_N}{S_N\sqrt{2\pi}}\exp\left[-\frac{1}{2}\left(\frac{\bar{\varepsilon}_m^{pl} - \varepsilon_N}{S_N}\right)^2\right] \quad (5)$$

where $\bar{\boldsymbol{\varepsilon}}_m^{pl}$ is equivalent plastic strain of the matrix, $\boldsymbol{\varepsilon}_N$ is mean strain at the micro-void nucleation, and S_N is the standard deviation. f_N is the volume fraction of tje voids, which are nucleated only when the tensile stress is applied. In this analysis, constants of the modified Gurson material model was determined from the tensile test result of SM490A steel[14]. The determined constants are as follows: q_1, q_2 and q_3 are 1.2, 0.7 and 1.44, respectively, and those are kept constant in the temperature range of the test; ε_N, S_N and f_N are 0.3, 0.1, and 0.04, respectively; initial volume fraction of micro-void is zero.

From the symmetry of the analysis, a half of the specimen is considered for the three-point bend and the compact tension test. The mesh models for both the specimens are shown in Fig.4. The fine mesh model used for near the crack tip for both the specimens is shown in Fig.5. The previous work[14] showed that if the inclusion is placed at certain distance from the crack tip, that is the average spacing of scatted inclusions, the analytical result well agreed with the experimental result. In this analysis, one inclusion of 5.0 μm in di ameter is placed at the position 100.0 μm distant from the crack tip. The mechanical property of the inclusion is the same as that of the matrix material. Variation in mechanical properties depending on the temperature, σ_Y, N, and C can be calculated for the temperature

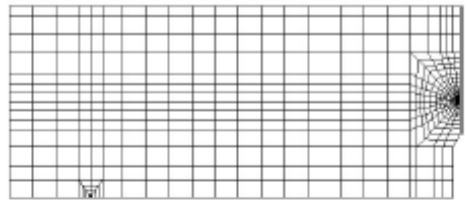

(a) Three-point bending specimen

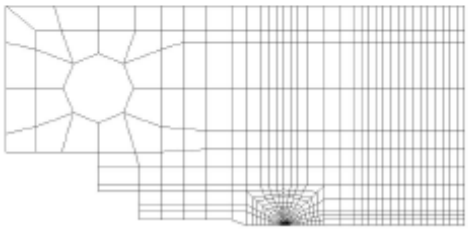

(b) CT specimen

Fig. 4 Finite element model

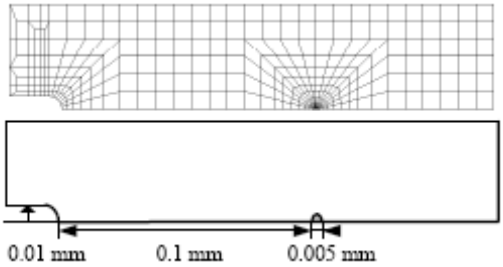

Fig.5 Finite element model around the crack tip

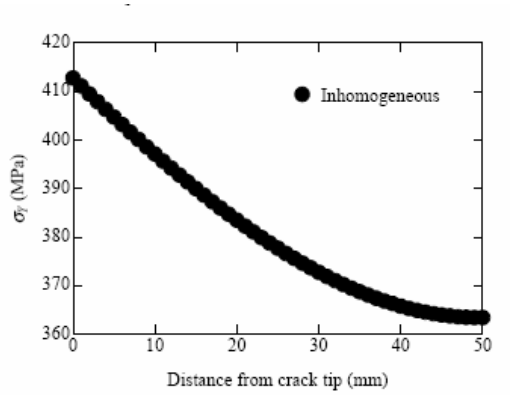

Φιγ. 6 Διστριβυτιον οφ ψιελδ στρεσσ σ_Y in the non-homogeneous model

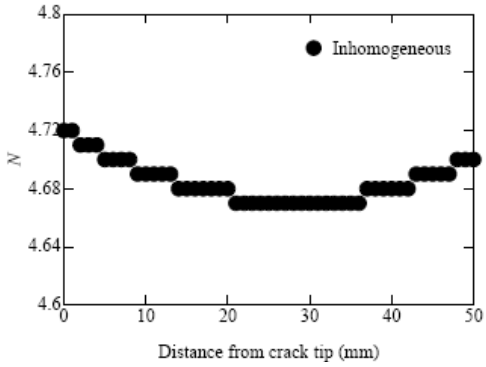

Fig. 7 Distribution of strain hardening exponent N in non-homogeneous model

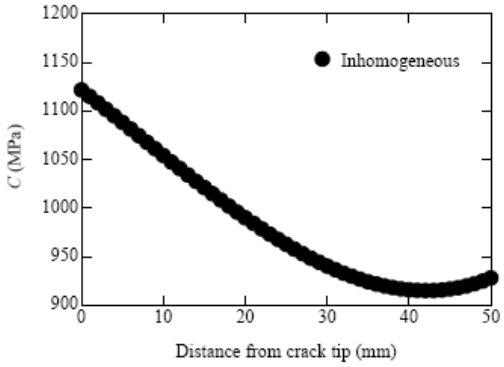

Fig. 8 Distribution of plastic coefficient C in the non-homogeneous model

gradient specimen and is shown in Figs. 6 to 8. These parameters are calculated by Eq (3) based on the temperature distribution measured by the experiment. In the analysis, the material property of each element is uniform within the element and determined by the temperature at the center of the element. Used mesh model is an eight-node isoparametric solid model with four integral points.

Fracture toughness is evaluated by J integral in the analysis. The J integral was calculated according to the experimental method used in the fracture toughness test. The commercial finite element code, ABAQUS was used for the analysis.

4.1 Analytical Results

The analytical result on the fracture toughness test at -45 ^{o}C uniform temperature showed that a dominant void was nucleated at the inclusion at the low level of the J integral and grew until cleavage fracture took place in the ligament between the dominant void and the crack tip at the J integral level of 39.0 kN/m. The estimated fracture toughness value, 39.0 kN/m falls in the region of cleavage fracture toughness shown in Fig.3.

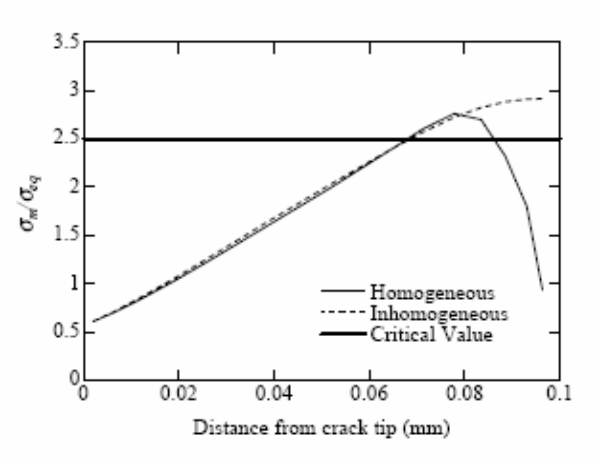

Fig. 9 σ_{yy} distributions ahead of crack tip for the homogeneous and the non-homogeneous model

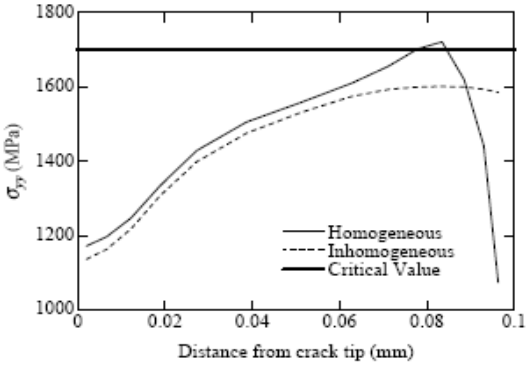

Fig. 10 σ_m/σ_{eq} distributions ahead of the crack tip for the homogeneous and the non-homogeneous model.

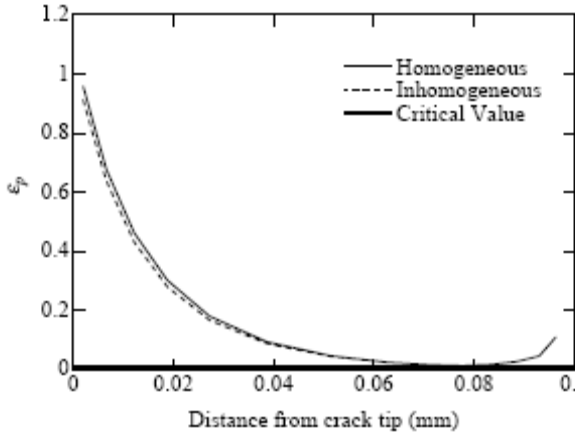

Fig. 11 ε_y distributions ahead of the crack tip for the homogeneous and the non-homogeneous model non-homogeneous model

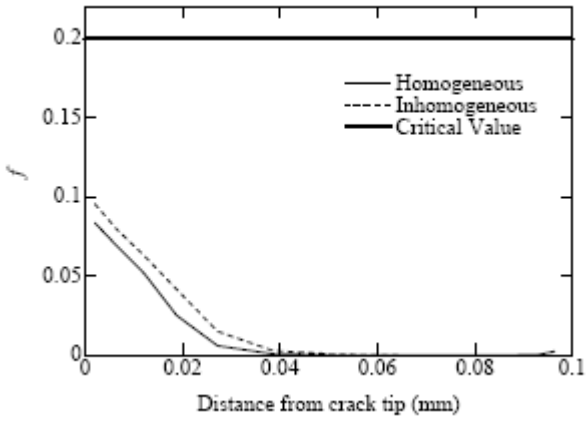

Fig.12 *f* distributions ahead of the crack tip for the homogeneous and the non-homogeneous model

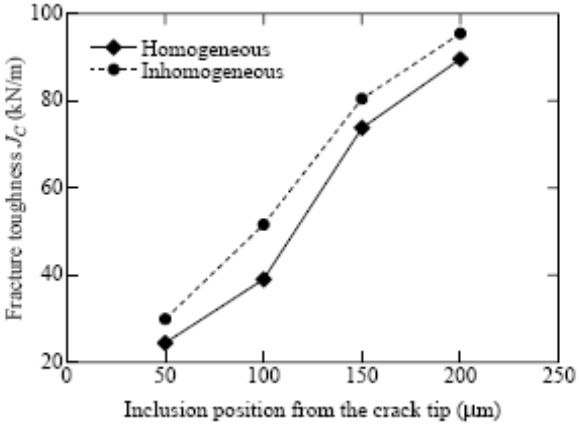

Fig. 13 Effect of inclusion position on the fracture toughness for the homogeneous and the non-homogeneous model

Fracture parameters, σ_{yy}, σ_m/σ_{eq}, and ε_p are plotted as a function of the distance from the crack tip in Figs. 9 to 11. There parameter values are calculated at the loading level associated with the fracture toughness of homogeneous model, $J_{C\text{-}Homo}$. It should be noticed that the distributions of these parameters are remarkably different of those for the homogeneous model at even the same J integral level. Steep decrease in the parameters σ_{yy}, and σ_m/σ_{eq} around 100 μm distant from the crack tip is caused by nucleation of a dominant void.

As seen in Fig. 9, the cleavage fracture criterion concerning the principal stress is not satisfied for the non-homogeneous model. Therefore, the further application of J integral beyond $J_{C\text{-}Homo}$ is necessary to satisfy the cleavage fracture criterion, so that fracture toughness of the non-homogeneous material will be enhanced. If the change in plastic parameters shown in Figs. 6 to 8 is examined within 100 μm distance from the crack tip, the largest change occurs in plastic coefficient C and it is less than 0.1 %. Therefore, the significant difference in fracture parameters between the homogeneous and the non-homogeneous model shown in Fig. 9 can be attributed to difference in the far field material property.

In the non-homogeneous model, the cleavage fracture criterion was satisfied after the J integral was enhanced up to 51.6 kN/m. The estimated fracture toughness value by this analysis falls within the range of the cleavage fracture toughness measured by the experiment as shown in Fig.3. The fracture toughness estimated in term of J integral for the non- homogeneous model induced by the temperature gradient increased by 32 % from the fracture toughness of the homogeneous model. In Fig.12, the void volume fraction is plotted as a function of the distance from the crack tip, when the applied load reaches fracture toughness for both the models. The micro voids are nucleated in the region of less than 40 μm distance from the crack tip, but the void volume fraction is not large enough to cause crack growth by a dimple fracture mode for both the homogeneous and the non-homogeneous model. This result well agrees with the experimental observation. In the above analysis, an inclusion is placed at the position equal to the average scattered spacing of inclusions from the crack tip. Effect of the inclusion position on the fracture toughness is examined in Fig. 13. The inclusion position is changed to 50, 150 and 200 μm distance from the crack tip. As the inclusion is placed away from the crack tip, the fracture toughness increases for both the homogeneous and non- homogeneous model. In addition, the apparent fracture toughness evaluated by J integral following the experimental method is greater for the non-homogeneous model than for the homogeneous for all the inclusion positions.

Through the numerical analysis results elaborated above, it should be noted that non-homogeneity in material property brings out the change in stress and strain fields ahead of the crack tip and eventually affects fracture toughness for the non-homogeneous material.

Conclusion

In this work, the material non-homogeneity was introduced by the temperature gradient in SM490A steel specimens and effect of material non-homogeneity on fracture toughness was investigated by an experiment and a numerical analysis. The following conclusions are obtained:

1. In this experiment, material non-homogeneity induced by temperature gradient influences the fracture toughness. Apparent fracture toughness evaluated by J integral experimentally measured for a non-homogeneous material is higher than that of a homogeneous material when ductile material property is assigned ahead of the crack tip.
2. Finite element analysis showed that the stress and the strain distribution ahead of the crack tip are different in the homogeneous and the non-homogeneous material at the same loading level.
3. Finite element analytical results can provide the reasonable explanation for the enhancement of the apparent fracture toughness in the non-homogeneous material.

6. References

Erdogan F., “Fracture mechanics of functionally graded materials.”, Composites Engineering, 5-7, (1995), pp.753–770

Delale F. and Erdogan F., “The crack problem for a nonhomogeneous plane.”, Journal of Applied Mechanics,50, (1983), pp.609–613

Eischen J.W., “Fracture of nonhomogeneous materials.”,International Journal of Fracture, 34, (1987), pp.3–22
Jin Z.-H. and Noda N., “Crack-Tip singular fields in nonhomogeneous materials.” Journal of applied Mechanics, 61, (1984), pp. 738-739
Konda N. and Erdogan F., “The mixed-mode crack problem in a nonhomogeneous elastic plane”, Engineering Fracture Mechanics, 47, (1994), pp.533–545
Erdogan F. and Wu B.H., “The surface crack problem for a plate with functionally graded properties.”, Journal of applied Mechanics, 64, (1997), pp.449–456
Anlas G., Santare M.H. and Lambros J., “Numerical calculation of stress intensity factors in functionally graded materials.”, International Journal of Fracture, 104,
(2000), pp.131–143
Kim J.-H. and Paulino G.H., “Finite element evaluation of mixed mode stress intensity factors in functionally graded materials.”, International Journal for Numerical Methods in Engineering, 53, (2002), pp.1903–1935
Dolbow J.E. and Gosz M., “On the computation of mixed-mode stress intensity factors in functionally graded materials.” International Journal of Solids and Structures, 39, (2002), pp.2557–2574
Rao B.N. and Rahman S., “Mesh-free analysis of cracks in isotropic functionally graded materials.”, Engineering Fracture Mechanics, 70, (2003), pp.1–27
Rousseau C.-E. and Tippur H.V., “Influence of elastic gradient profiles on dynamically loaded functionally graded materials: cracks along the gradient.”, International Journal of Solids and Structures, 38, (2001), pp.7839–7856
Homma H., Shah Q.H. and Kawada S., “Effect of temperature gradient on crack initiation.”, The International Journal of Pressure Vessels and Piping, 63-3, (1995), pp.339–345
Nakamoto H., Homma H., Suzuki S., and Kusutani S., “Prediction of fracture toughness in ductile-brittle transition region.” Transaction of JSCES, Paper No.2004007 (2004)
Wang G.Z., Liu G.H. and Chen J.H., “Effects of precracked specimen geometry on local cleavage fracture stress σ_f of low alloy steel.”, International Journal of Fracture, 112, (2001), pp.183–196
Tvergaard V., “Influence of voids on shear band instabilities under plane strain conditions.”, International Journal of Fracture, 17, (1981), pp.389–407
Tvergaard V., “On the localization in ductile materials containing spherical voids.”, International Journal of Fracture, 18, (1982), pp.237–252
Hibbitt, Karlsson & Sorensen, Inc., “ABAQUS users and theory manual, version 6.2.”, (2002), Providence, RI.